Solid State Communications 195 (2014) 26–30

Contents lists available at ScienceDirect

Solid State Communications

journal homepage: www.elsevier.com/locate/ssc

Structural and mechanical properties of GaAs under pressure up to 200 GPa

Prayoonsak Pluengphon [a,*], Thiti Bovornratanaraks [b,c], Sornthep Vannarat [d], Udomsilp Pinsook [b,c]

[a] Division of Physical Science, Faculty of Science and Technology, Huachiew Chalermprakiet University, Samutprakarn 10540, Thailand
[b] Extreme Conditions Physics Research Laboratory, Department of Physics, Faculty of Science, Chulalongkorn University, Bangkok 10330, Thailand
[c] ThEP Center, CHE, 328 Si-Ayuttaya Road, Bangkok 10400, Thailand
[d] Large-Scale Simulation Research Laboratory, National Electronics and Computer Technology Center, Pathumthani 12120, Thailand

ARTICLE INFO

Article history:
Received 8 February 2014
Received in revised form
28 May 2014
Accepted 22 June 2014
by H. Akai
Available online 27 June 2014

Keywords:
A. GaAs
B. *Ab initio* calculation
D. High pressure
D. Transformation path

ABSTRACT

Ab initio calculations were performed for investigating the high pressure phases of GaAs up to 200 GPa. By comparing the minimum free energies of structures, we found the thermodynamically stable phases of GaAs under pressure beyond GaAs-III (*Imm2*) with space groups *Pmma* and *P4/nmm* at the pressure range of 88–146 GPa and 146–200 GPa, respectively. For discussing the difference results of GaAs IV and V in previous studies, we found that *Pmma* and *P4/nmm* are the lower symmetric phases of *P6/mmm* and *CsCl-like*, respectively. For analyzing the *Pmma*→*P4/nmm* phase transition, we observed the approximated path and found that the barrier of transformation from *Pmma* to *P4/nmm* in direction [110] is 0.035 eV. The graph of density of states shows no energy gap in stable phases at 130 and 160 GPa, indicating that *Pmma* and *P4/nmm* are the metallic phases. The contour plots of the electron density difference show some valence electron sharing in *Pmma* which is higher than in *P4/nmm*. Moreover, the results of elastic parameters and modulus ratio suggested that the *Pmma* phase is a ductile material, while the *P4/nmm* phase is a brittle due to the increasing of shear modulus.

1. Introduction

Gallium arsenide (GaAs) which is one of III–V binary compound semiconductors is widely used in many applications such as solar cell fabrications and diode devices. Stable phase at ambient pressure of GaAs is the zinc blende (*ZB*) phase (space group *F-43m*), which is similar to the other III–V binary compounds such as GaP, InP and InAs [1]. In previous studies of GaAs high-pressure phases, it has been suggested that GaAs–*ZB* transforms to an orthorhombic phase near 17 GPa [2,3]. By studying the X-ray-diffraction pattern from synchrotron radiation, Weir et al. [4] suggested that the evolution of GaAs structures under high pressure is the following: GaAs-I (*ZB*)→GaAs-II (*Pmm2*)→GaAs-III (*Imm2*)→GaAs-IV (*P6/mmm*), with the transitions pressures of 17, 24, and 60 GPa, respectively. The simple hexagonal phase (space group *P6/mmm*) in GaAs-IV from the experiment is similar to the ambient pressure phase of GaSb [5,6]. Zhang and Cohen [7] studied the equilibrium lattice parameters and internal parameters of GaAs-II by using *ab initio* pseudopotential calculations within the local density functional (LDA) in the form of Perdew and Zunger. They found that GaAs-II is orthorhombic structure which is thermodynamically favored over the rocksalt ($Fm\bar{3}m$) structure. Later, McMahon and Nelmes [8] used the angle-dispersive powder diffraction technique and confirmed that the structure of GaAs-II is a *Cmcm* space group. Mujica and Needs [9] using first principle calculations confirmed that GaAs-II in *Cmcm* structure is more stable than *Pmm2*. Durandurdu and Drabold [10] performed a local-orbital quantum molecular dynamic method with a 216-atom model of GaAs. They used norm-conserving pseudopotentials and Harris functional, and found that the GaAs *ZB* phase transforms to *Cmcm* at 23.5 GPa, and *Cmcm* phase changes to *Imm2* structure at 57 GPa. From the study of the electronic density of states (EDOS), they concluded that both *Cmcm* and *Imm2* phases of GaAs are semimetals. The stability of vibration modes in both high-pressure phases was confirmed by studying the phonon density of states (PDOS). For very high pressure phases (> 80 GPa), Garcia and Cohen [11] studied the *3d* states in Ga compounds with core relaxation effects and predicted that body-centered cubic structure should be stable phase of GaAs above 125 GPa. However, Kim et al. [12] suggested the instability of the *CsCl-like* structure (space group *Pm-3m*) in most III–V semiconductors by using the density-functional linear response method. They focused on InP and InSb in the normalize volume (V/V_0) in range 0.55–0.40. They concluded that the ionic

* Corresponding author.
E-mail address: prayoonsak@gmail.com (P. Pluengphon).

http://dx.doi.org/10.1016/j.ssc.2014.06.016
0038-1098/

compounds such as GaP, GaAs, InP, and InAs are dynamically unstable at high pressures with respect to transverse-acoustic phonon. They suggested two candidate structures that replaced the *CsCl-like* structure at very high pressure are *P4/nmm* and *Pmma*.

From the literature reviews, the theoretical and experimental investigations of GaAs in I, II and III phases under high pressure have been widely conducted. However, the studies of structural and mechanical properties under extremely high pressure (80–200 GPa) in GaAs-IV and V phases are not yet completed. In this work, the thermodynamic stability of GaAs in IV and V phases are discussed up to 200 GPa. The relations of similar structures (*Pmma-P6/mmm* and *P4/nmm-CsCl-like*) were explained. We predicted the mechanism of path transformation in GaAs from *Pmma* to *P4/nmm* which is well above the experimental observation. In order to analyze the physical properties of GaAs IV and V, the elastic parameters, namely, the bulk modulus and shear modulus are studied to classify the metallization of the phases IV and V.

2. Calculation details

In this work, the *ab initio* calculations are performed based on the density functional theory (DFT) as implemented in the CASTEP code [13,14]. In DFT, all ground states properties of a solid system such as the electron density, effective potential and total energy were evaluated by self-consistently solving the Kohn–Sham equations. First of all, the exchange–correlation functionals which contained in Kohn–Sham equations were observed by comparing the results with the previous experiments. At ambient pressure condition (0 GPa), the cutoff energy and k-point grid were used at 500 eV and $6\times6\times6$, which gave the energy convergence at 5 meV/atom. The lattice parameters ($a=b=c$) in *ZB* at ambient pressure were determined as 5.576 and 5.729 Å by using the LDA functional and the generalizaed-gradient approximation of Perdew–Burke–Ernzerhof (GGA-PBE) functionals [15–17]. Bulk modulus of GaAs from the experiments [18,19] is 74.7 GPa, while the calculation results are 75.5 GPa (LDA) and 60.3 GPa (GGA-PBE) as shown in Table 1.

From Table 1, we found that the LDA functional gives a better agreement with the experimental results than the GGA-PBE. The LDA functional was therefore selected for the rest of this study. The ultrasoft pseudopotentials that included the electronic configurations $3d^{10}4s^24p^1$ for Ga and $4s^24p^3$for As were used. The cutoff energy of 500 eV was found to be suitable for calculating the geometry optimizations, single point energies and elastic parameters. Forces on the optimized atomic positions were calculated by using the Hellmann–Feynman theorem [20]. The Brouillion zone integration was performed using the Monkhorst–Pack grids [21] of $6\times6\times6$ for *ZB*, $10\times10\times8$ for *Cmcm*, $12\times12\times10$ for *Imm2*, $10\times10\times5$ for *P6/mmm*, $10\times10\times10$ for *CsCl-like* and $6\times6\times11$ for *P4/nmm* and *Pmma* structures. These were sufficient to converge the total energies to within 5 meV per atom for all structures. For the example of study the effect of k-point on the wide pressure range, the Fig. 1 shows the k-point of the example structure (*CsCl-like*) in the pressure 120, 160 and 200 GPa. The total energies confirmed that the k-point set $10\times10\times10$ which was used to calculate in *CsCl-like* still converges in this pressure range. The total energies in the wide pressure range were observed and found that these k-point sets still converge in this pressure range. However, the k-point in a direction (k) of some space groups was carefully varied under wide pressure range by controlling actual spacing ($1/k$) at about 0.04 Å in all dimensions (x, y and z).

Table 1
The lattice parameter and bulk modulus of GaAs–*ZB* at ambient pressure from DFT calculations compared with the previous experiments [18,19].

Parameter/Method	Exp.	LDA	GGA-PBE
Lattice parameter (Å)	5.653 (Ref. [18])	5.576	5.729
Bulk modulus GPa	74.7 (Ref. [18,19])	75.5	60.3

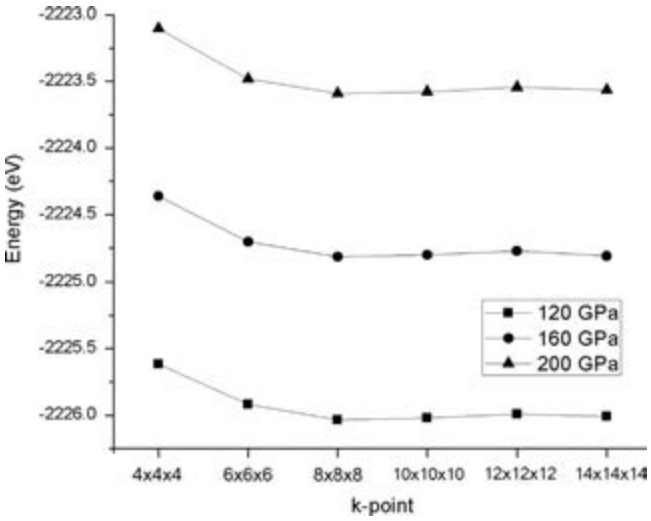

Fig. 1. Graph of total energy (y-axis) and k-point (x-axis) of GaAs in the example (*CsCl-like*) structure shows that the total energies converged at k-point set $8\times8\times8$ in a wide pressure range (120–200 GPa).

3. Results and discussion

For finding the mechanism of GaAs phase transitions, we optimized the possible space groups to find the total energy per primitive cell (E) and their volume (V) at a given pressure (P). The total energies of GaAs structures in *ZB*, *Fm-3m*, *Cmcm*, *Cinnabar* ($P3_121$), *Imm2*, *P6/mmm*, *CsCl-like*, *P4/nmm* and *Pmma* were observed. *E–V* curves were fitted by using the third order Birch–Murnaghan equation of state [22,23]. For analyzing phase stabilities, the enthalpy (H) per a formula unit of a GaAs space group was calculated from the relation $H=E+PV$, which is the free energy of system at 0 K. The enthalpies of GaAs structures were compared under pressure up to 200 GPa. The *Fm-3m* structure has also been observed with remarkably higher in energy compared to the *ZB* (about 4 eV). Our calculation found that the *Cinnabar* and *Fm-3m* phases are not stable structures under this condition (0 K) because *ZB* transforms directly to the *Cmcm* without going through the *Cinnabar* phase that has the higher free energy (>1 eV). We found the minimum enthalpy structures between 0 and 200 GPa as shown in Fig. 2, which consist of GaAs I-*ZB* (0–12 GPa), GaAs II-*Cmcm* (12–37 GPa), GaAs III-*Imm2* (37–88 GPa), GaAs IV-*Pmma* (88–146 GPa) and GaAs V-*P4/nmm* (146–200 GPa), respectively. Therefore, for lower pressure range, we report the transition sequence from *ZB*→*Cmcm*→*Imm2* which confirmed Durandurdu and Drabold's work [10]. We found that the enthalpy of *ZB* compared to the *Cmcm* and the volume reduction during the *ZB-Cmcm* phase transition is larger than those of the *Cmcm-Imm2*. This can be understood since the *ZB* to *Cmcm* transition is a structural reconstruction, but *Cmcm-Imm2* transition is a distortion from the orthorhombic structure.

Under extremely high pressure ($P>80$ GPa), we found that *Imm2* changes to the *Pmma* space group with atomic positions Ga (0.25, 0.00, 0.75) and As (0.25, 0.50, 0.75) at 88 GPa which confirms the suggestion of Kim et al. [12]. However, the experiment of

Weir et al. [4] suggested that GaAs-IV is *P6/mmm*. Therefore, we also analyze the relation of 2 space groups between *Pmma* and *P6/mmm*. In Table 2, atomic positions of Ga and As in *Pmma* were compared with the primitive basis of *P6/mmm* at the same pressure. We found that the *Pmma* in GaAs is the similar structure with *P6/mmm* but it has lower symmetry than *P6/mmm*; as a result, *Pmma* gave lower free energies in all pressure as shown the *H-P* curves in Fig. 2. In addition, the Fig. 2 indicated that the *P4/nmm* structure is the thermodynamically stable phase above *Pmma* ($P > 146$ GPa) in good agreement with Kim *et al.* suggestion [12]. We found that the atomic positions of Ga (0.00, 0.00, 0.00) and As (0.00, 0.50, z) give minimum free energy in *P4/nmm* structure at $z=0.498$. At a constant pressure (such as 140 GPa), the enthalpy difference (such as between *Pmma* and *P6/mmm* structures) is about 0.025 eV per a GaAs formula unit (see in Fig. 2), while the accuracy of energy calculation is 0.010 eV per formula unit of GaAs. We found that the tiny differences of free energies are larger than the error of energy calculations. Therefore, we can separate the distinguish structures between *Pmma* and *P6/mmm*. When we analyze atomic positions of *P4/nmm* compared with the primitive basis of *CsCl-like* space group as shown in Table 2, we concluded that *P4/nmm* structure in stable condition is similar to *CsCl-like* structure.

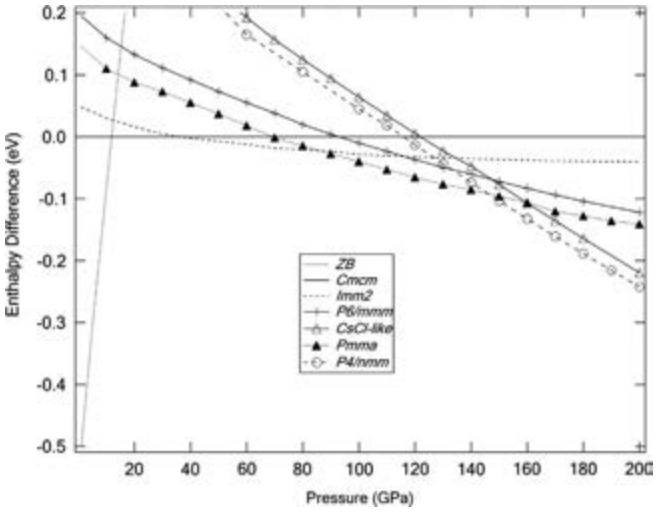

Fig. 2. The enthalpy difference of GaAs high-pressure phases compared with the enthalpy's *Cmcm* phase.

In Fig. 3, we explore the nature of *Pmma*→*P4/nmm* transition mechanism. In the similar method that we have reported in $CuInSe_2$ [24] and $Cu(In,Ga)Se_2$ [25], we analyze the transformation path between two phases as follows. Firstly, we investigate the transition pressure of *Pmma*→*P4/nmm* which was predicted at 146 GPa where the enthalpy of two structures are equal. Secondly, we analyze the transformation path from *P6/mmm* structure. We knew that the atomic positions in *P4/nmm* at minimum free energy are the distorted structure from *CsCl-like*. We estimate that the As-plane was shifted from Ga-plane in direction [110] and the space group of GaAs was changed from *Pmma*, shown in Fig. 3(a). Lattice parameters and angles in the unit cell were optimized and controlled the pressure at 146 GPa. We found that the enthalpy of system increases along the distance of As-plane from Ga-plane. Finally, the As-plane was shift to the center of unit cell; as a result, the space group was change to *P4/nmm*. The barrier of free energy in *Pmma*→*P4/nmm* is estimated to be 0.035 eV per formula unit of GaAs, this approximate path shown in Fig. 3.

In addition, we would like to explain the extensive detail on the metallization of GaAs in *Pmma* and *P4/nmm* phases. In Fig. 4, we

Table 2
Atomic positions and lattice parameters in *Pmma* and *P4/nmm* at 146 GPa when were compared with the primitive basis of space groups *P6/mmm* and *CsCl-like*, respectively.

Space group	Lattice parameters	Angles	Ga	As
P6/mmm	(2.336,2.336,4.356)	(90,90,120)	(0,0,0)	(0,0,0.50)
Pmma (in basis *P6/mmm*)	(2.331,2.345,4.353)	(90,90,119.7)	(0,0,0)	(0,0,0.50)
CsCl-like	(2.728,2.728,2.728)	(90,90,90)	(0,0,0)	(0.50,0.50,0.50)
P4/nmm (in basis *CsCl-like*)	(2.775,2.775,2.629)	(90,90,90)	(0,0,0)	(0.50,0.50,0.50)

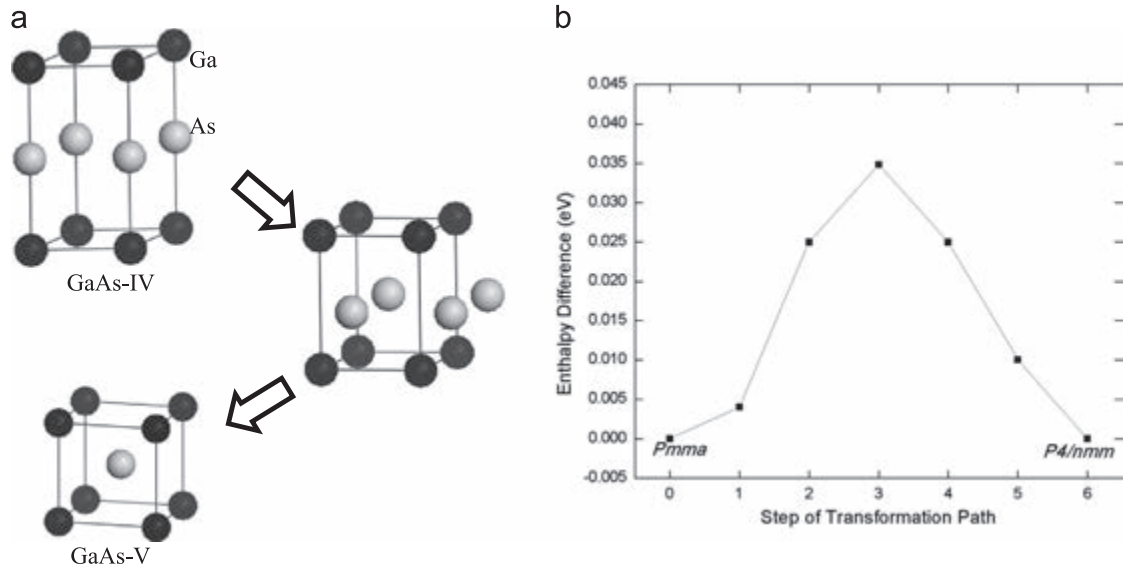

Fig. 3. (a) The simple model of structural evolution during the phase transition from *Pmma* to *P4/nmm* phases in direction [110] was estimated. (b) The enthalpy barrier during phase transformation from GaAs IV to GaAs V at 146 GPa in this estimated path is 0.035 eV.

compared the electronic density of states (EDOSs) of GaAs in *ZB* (0 GPa), *Imm2* (50 GPa), *Pmma* (130 GPa) and *P4/nmm* (160 GPa) structures. The EDOSs show that GaAs–*ZB* at 0 GPa is a semiconductor as it has an energy gap, GaAs-*Imm2* at 50 GPa is a semimetal in agreement with the previous suggestion of Durandurdu and Drabold [10]. In *Pmma* and *P4/nmm* phases, the graphs of EDOSs are continuous along the energy axis, thus they are in the metallic phases. For studying the chemical bonding, we calculated the electron density difference in the high pressure phases, *i.e. Pmma* (130 GPa) and *P4/nmm* (160 GPa) and the results are shown in Fig. 5. The contour plots show the difference of electron densities (between −0.1 and 0.3) from the chemical bonding in each GaAs lattice, relative to electron densities in isolate atoms. The electron density difference of GaAs is the difference between the electron density of the total GaAs system and the unperturbed electron densities of Ga and As. The electron density difference shows the changes in the electron distribution due to the formation of all chemical bonds. It is useful for illustrating how chemical bonds are formed across the whole system as the electron density difference can help identifying the types of chemical bonds, such as covalent bonding, metallic bonding *etc.* These show that the chemical bonding in *Pmma* has higher electron sharing (orange and yellow zone) at cavity between Ga (gray ball) and As (violet ball) compared with in *P4/nmm*. Therefore, the covalent bonding in *Pmma* is higher than in *P4/nmm*. However, we found from the results of total electron density difference that high electron sharing in *Pmma* is anisotropy due to appearing in any planes while it is not found in all planes of *P4/nmm*. The plane of high electron sharing in *Pmma* is shown in Fig. 5. The covalent bond was found in some planes of *Pmma*, but EDOS and band structure which indicate the macroscopic properties of system show that *Pmma* is the metallic phase. By studying the population analysis and Hirshfeld charges, it confirmed that the ionic charge in *P4/nmm* is higher than in *Pmma*. The covalent bond does not necessarily appear only in insulator. For example, the bonds in some metals such as $BeCl_2$, $SnCl_2$ and $SnCl_4$ are covalent bonds at ambient pressure but these materials can have free electrons as well. In GaAs-*Pmma*, the difference of the electronegativity between Ga and As is less than of Be and Cl; therefore, it is possible to have the covalent bond in *Pmma* phase. The chemical bonds in *Pmma* and *P4/nmm* excited the population of Ga ($3d^{10}4s^24p^1$) and As ($3d^{10}4s^24p^3$), which the states 4s transformed to 4p (*s* to *p*). The elastic properties such as elastic constants (C_{ij}), bulk modulus (B) and shear modulus (G) were studied for determining the physical properties of GaAs in *Pmma* and *P4/nmm* phases. At the beginning, the elastic parameters in ambient pressure phase were observed by using LDA functional as shown in Table 3. We found that the LDA functional gives a good agreement with the previous experiments [18,19,26] more than using GGA-PBE. The elastic properties of materials can be estimated by using the Voigt–Reuss–Hill procedure [27–29]. Voigt and Reuss equations are the upper and lower limits of true crystalline constants, while the mean value from the Voigt (B_V, G_V) and Reuss (B_R, G_R) approximation is the Hill (B_H, G_H) modulus. In this work, the Hill modulus of GaAs is reported as shown in Table 3. For analyzing type of material, it is classified as brittle material if the ratio of B/G less than 1.75, and it is a ductile material when the ratio greater than 1.75 [30,31]. Shear modulus of GaAs increases highly when *Pmma* changes to *P4/nmm*. GaAs- *P4/nmm* increases the resistance from the tangential force. From the B/G ratio in Table 3, we can conclude that GaAs in *Pmma* phase is ductile material, while *P4/nmm* phase is a brittle.

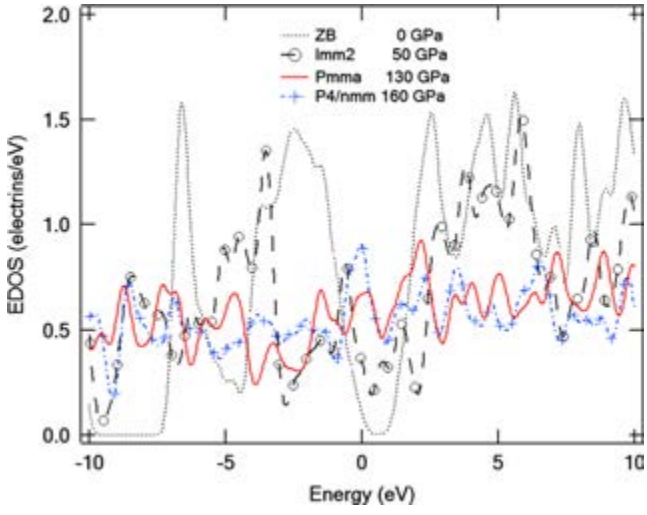

Fig. 4. (Color online) Comparisons of the electronic density of states of GaAs in *ZB* (0 GPa), *Imm2* (50 GPa), *Pmma* (130 GPa) and *P4/nmm* (160 GPa) structures.

4. Conclusions

We performed *ab initio* calculations in CASTEP code for studying the transitions pressure and stability of high pressure phases of

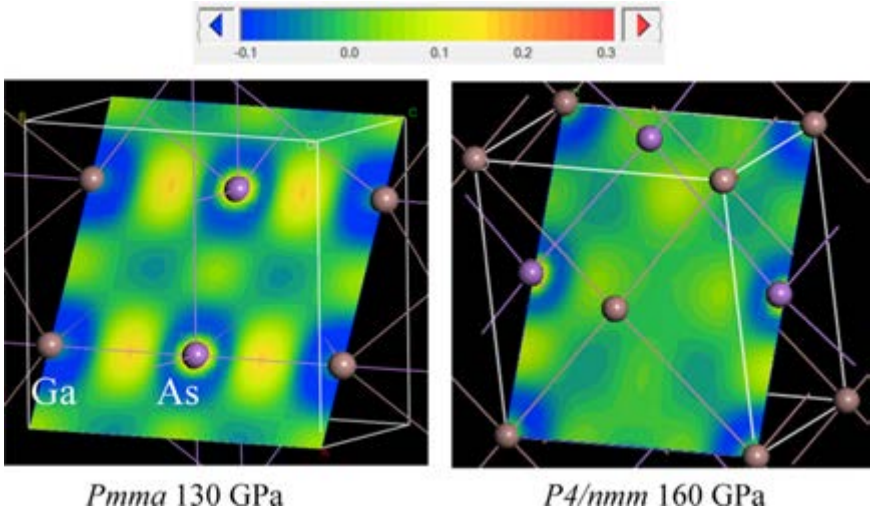

Fig. 5. (Color online) Comparison of the electronic density difference (the value between −0.1 and 0.3) of GaAs in *Pmma* (130 GPa) and *P4/nmm* (160 GPa) structures.

Table 3
Elastic parameters in a unit GPa of GaAs–*ZB* (0 GPa), GaAs-*Pmma* (100, 120 and 145 GPa) and GaAs-*P4/nmm* (160, 170, 180 and 200 GPa).

Phase	*P* (GPa)	C_{11}	C_{12}	C_{13}	C_{23}	C_{22}	C_{33}	C_{44}	C_{55}	C_{66}	*B*	*G*	*B/G*
ZB	0	120	53	53	53	120	120	62	62	62	75	48	1.56
Pmma	100	958	121	279	157	1080	1010	120	264	67	462	157	2.94
	120	1073	145	320	199	1230	1135	121	292	69	529	163	3.25
	145	1165	109	505	298	1413	1168	148	364	69	615	174	3.53
P4/nmm	160	1265	295	403	403	1265	1148	432	432	415	653	425	1.54
	170	1323	310	427	427	1323	1188	449	449	418	685	438	1.56
	180	1380	325	454	454	1380	1228	469	469	421	717	451	1.59
	200	1489	353	510	510	1489	1307	512	512	430	781	477	1.64

GaAs between 0 and 200 GPa. The stability of GaAs structures were considered by comparing the minimum free energy or enthalpy of system. From observation by using LDA functional, we found that the high-pressure phases of GaAs are *ZB* (0–12 GPa), *Cmcm* (12–37 GPa), *Imm2* (37–88 GPa), *Pmma* (88–146 GPa) and *P4/nmm* (146–200 GPa), respectively. The difference results from theoretical and experimental reports were concluded that *Pmma* and *P4/nmm* are the distorted structures of *P6/mmm* and *CsCl-like*, respectively. The lower symmetric phases gave the minimum free energies in Fig. 2. Transformation path from *Pmma* to *P4/nmm* phases was estimated and found that *P6/mmm* changes to *P4/nmm* in direction [110]. The enthalpy barrier of this path is 0.035 eV. In addition, physical properties of the metallic phases GaAs were examined by analyzing the elastic parameters. The continuous of EDOSs show the metallization of *Pmma* and *P4/nmm* phases. The electron density difference contour plots show that the sharing electron in *Pmma* is higher than in *P4/nmm*. This indicates that *Pmma* has the characteristic of the covalent bond. From the modulus ratio, it can be concluded that *Pmma* phase is a ductile material, while the *P4/nmm* phase is a brittle.

Acknowledgments

P. Pluengphon would like to acknowledge the research funding from Faculty of Science and Technology, Huachiew Chalermprakiet University. T. Bovornratanaraks acknowledges the financial support from Asahi Glass Foundation, National Research Council of Thailand, Thailand Research Fund contract number RSA5580014. Computing facilities are supported by the Ratchadaphiseksomphot Endowment Fund (RES560530180-AM) and the Special Task Force for Activating Research (STAR), Ratchadaphiseksomphot Endowment Fund, Chulalongkorn University, through the Energy Material Physics Research Group.

References

[1] A. Mujica, A. Rubio, A. Munoz, R.J. Needs, Rev. Mod. Phys. 75 (2003) 863.
[2] S.C. Yu, I.L. Spain, E.F. Skelton, Sol. Stat. Commun. 25 (1978) 49.
[3] M.A. Baublitz, A.L. Ruoff, J. Appl. Phys. 53 (1982) 6179.
[4] S.T. Weir, T.K. Vohra, C.A. Vanderborg, A.L. Ruoff, Phys. Rev. B 39 (1989) 1280.
[5] S.B. Zhang, M.L. Cohen, Phys. Rev. B 35 (1987) 7604.
[6] S.T. Weir, Y.K. Vohra, A.L. Ruoff, Phys. Rev. B 36 (1987) 4543.
[7] S.B. Zhang, M.L. Cohen, Phys. Rev. B 39 (1989) 1450.
[8] M.I. McMahon, R.J. Nelmes, Phys. Status Solidi B 198 (1996) 389.
[9] A. Mujica, R.J. Needs, J. Phys.: Cond. Matt 8 (1996) L237.
[10] M. Durandurdu, D.A. Drabold, Phys. Rev. B 66 (2002) 045209.
[11] A. Garcia, M.L. Cohen, Phys. Rev. B 47 (1993) 6751.
[12] K. Kim, V. Ozolins, A. Zunger, Phys. Rev. B 60 (1999) R8449.
[13] M.C. Payne, M.P. Teter, D.C. Allan, T.A. Arias, D. Joannopoulos, Rev. Mod. Phys. 64 (1992) 1045.
[14] M.D. Segall, P.L.D. Lindan, M.J. Probert, C.J. Pickard, P.J. Hasnip, S.J. Clark, M. C. Payne, J. Phys.: Condens. Matt 14 (2002) 2717.
[15] J.P. Perdew, A. Zunger, Phys. Rev. B 23 (1981) 5048.
[16] J.P. Perdew, K. Burke, M. Ernzerhof, Phys. Rev. Lett. 77 (1996) 3865.
[17] J.P. Perdew, J.A. Chevary, S.H. Vosko, K.A. Jackson, M.R. Pederson, D.J. Singh, C. Fiolhais, Phys. Rev. B 46 (1992) 6671.
[18] S. Saib, N. Bouarissa, Sol. Stat. Electron. 50 (2006) 763.
[19] McSkimin, H.J. Jayaraman, A. Andreatch, P. Bell, J. Appl. Phys. 38 (1967) 2362.
[20] R.P. Feynman, Phys. Rev 56 (4) (1939) 340.
[21] H.J. Monkhorst, J.D. Pack, Phys. Rev. B 13 (1976) 5188.
[22] F. Birch, Phys. Rev 71 (1947) 809.
[23] F.D. Murnaghan, Proc. Natl. Acad. Sci. 30 (1944) 244.
[24] P. Pluengphon, T. Bovornratanaraks, S. Vannarat, K. Yoodee, D. Ruffolo, U. Pinsook, Sol. Stat. Commun. 152 (2012) 775.
[25] P. Pluengphon, T. Bovornratanaraks, S. Vannarat, U. Pinsook, J. Phys.: Condens. Matter 24 (2012) 095802.
[26] A.M. Teweldeberhan, J.L. Dubois, S.A. Bonev, Phys. Rev. Lett. 105 (2010) 235503.
[27] W. Voigt Lehrbuch der Kristallphysik (Teubner:Leipzig) 716, 1928 (in German).
[28] A. Reuss, Z. Angew, Math. Mech. 9 (1929) 49.
[29] R. Hill, Proc. Phys. Soc. A 65 (1952) 349.
[30] S.F. Pugh, Phil. Mag. 45 (1953) 833.
[31] M. Aftabuzzaman, A.K.M.A. Islam, J. Phys.: Condens. Matter 23 (2011) 105701.